

# A New Non-Gaussian Performance Evaluation Method in Uncompensated Coherent Optical Transmission Systems

Seyed Sadra Kashef \*

Faculty of Electrical and Computer Engineering, Urmia University, Iran  
s.kashef@urmia.ac.ir

Paeiz Azmi

Faculty of Electrical and Computer Engineering, Tarbiat Modares University, Iran  
pazmi@modares.ac.ir

Received: 04/Jul/2019

Revised: 24/Oct/2019

Accepted: 20/Dec/2019

## Abstract

In this paper, the statistical distribution of the received quadrature amplitude modulation (QAM) signal components is analyzed after propagation in a dispersion uncompensated coherent optical fiber link. Two Gaussian tests, the Anderson-Darling and the Jarque-Bera have been used to measure the distance from the Gaussian distribution. By increasing the launch power, the received signal distribution starts to deviate from Gaussian. This deviation can have significant effects in system performance evaluation. The use of the Johnson  $s_U$  distribution is proposed for the performance evaluation of orthogonal frequency division multiplexing in an uncompensated coherent optical system. Here, the Johnson  $s_U$  is extended to predict the performance of multi-subcarrier and also single carrier systems with M-QAM signals. In particular, symbol error rate is derived based on the Johnson  $s_U$  distribution and performance estimations are verified through accurate Monte-Carlo simulations based on the split-step Fourier method. In addition, a new formulation for the calculation of signal to noise ratio is presented, which is more accurate than those proposed in the literature. In the linear region, the Johnson based estimations are the same as Gaussian; however, in the nonlinear region, Johnson  $s_U$  distribution power prediction is more accurate than the one obtained using the Gaussian approximation, which is verified by the numerical results.

**Keywords:** Coherent optical fiber link; Gaussian distribution; Johnson  $s_U$  distribution; nonlinear transmission performance; Uncompensated Transmission; QPSK.

## 1- Introduction

Modeling of nonlinear propagation in coherent optical communication systems is of fundamental to predict system performance. In particular, [1], [2], [3] present a practical survey on modeling of nonlinear propagation in uncompensated transmission (UT) systems. Although, the propagation of light in optical fiber channels is properly modeled by the non-linear Schrodinger equation, it is difficult to attain an accurate statistical model of nonlinear fiber channel [4] because of the non-Gaussian behavior of noise [5].

In this context, the Gaussian-Noise model (GN-model) is known as an accurate and acceptable reference model that is applied in different system scenarios for coherent optical communication. This model has been successfully used in system design, analysis and network optimization. However, in some scenarios such as strong nonlinear propagation and low dispersion the accuracy of the GN-model is reduced. Therefore, various models with higher accuracy have been suggested in many different scenarios [6], [7], [8].

In long-haul propagation, amplified spontaneous emission (ASE) noise and nonlinear interference (NLI) caused by the Kerr effect are pointed out as the two main system impairments [5]. As demonstrated in [9], the use of an inaccurate signal statistic can give more than 500 km error in reach prediction of a fiber-optic transmission system. This statistical deviation of received signal histogram from Gaussian distribution is measured using two powerful tests named Kolmogorov-Smirnov and Anderson-Darling (AD) [10], [11] and is shown in different scenarios.

To overcome the inaccuracy of Gaussian distribution, some enhanced methods have been introduced in [12] to improve the accuracy of the GN model. In some cases, a correction factor has been applied to achieving more accuracy in different systems, like coherent optical orthogonal frequency-division multiplexing (CO-OFDM) [10], [13], [14].

The much of the literature is focused on calculating the moments of propagated signal based on a simple Gaussian assumption, which requires the estimation of just one moment (the variance). However, the non-Gaussian distribution of the signal after highly nonlinear propagation is not compliant with this assumption and the

\* Corresponding Author

estimation of higher moments of the received signal statistics is required, it as shown in [11]. The Non-Gaussian behavior of propagated signal is included in an enhanced version of the GN model, named EGN, that takes into account for high order moments of the signal [15]. The Gaussian assumption of the received signal starts to be inaccurate at the nonlinear threshold, as shown in [11]. The typical operating parts of optical systems fall around this threshold. Therefore, an accurate model in this region can play an important role.

The use of Johnson  $s_U$  distribution for BER calculation was proposed for the first time in [11], [16] in CO-OFDM system with different modulations. The accuracy of the Johnson  $s_U$  based methods were verified using both analytical and numerical results. The study presented in this article seeks to further extend the use of the Johnson  $s_U$  distribution statistic for the performance evaluation of other coherent optical UT systems with different kinds of modulation and signals ([11] and [16] were only focused on OFDM signals) which is presented in [17], briefly. Single carrier M-QAM signals are the first aim; next, multi-subcarrier (MSC) QPSK transmission systems are considered because of their higher nonlinear robustness [18/], [19/], [20/], [21/]. We also analyzed the performance of proposed method in dual polarization systems.

Therefore, we investigate the Gaussian assumption accuracy of the propagated signal components in different modulation and signals to extend Johnson  $s_U$  distribution applications. The deviation of nonlinear noise pdf from Gaussian is measured using two well-known pdf tests, namely, Jarque-Bera (JB) and AD. Johnson  $s_U$  pdf includes higher-order statistics to achieve a more accurate prediction. We report the obtained SER through direct error counting in the Monte-Carlo (MC) simulation based on the split-step Fourier method (SSFM), and the difference from (a) the GN-model based SER estimation and (b) Johnson  $s_U$  based method.

The rest of the paper is organized as follow. Section 2 describes the system model which section 3 introduces the Mathematical Preliminaries of system performance evaluation through UT over fiber optic. The statistical features of propagated signal is evaluated and Johnson  $s_U$  pdf is suggested for more accuracy. Finally, Johnson  $s_U$  is applied for BER evaluation in Section 4. Conclusions are presented in Section 5.

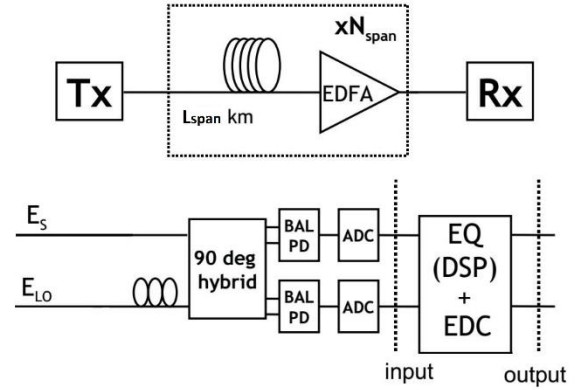


Fig. 1 Top: link structure. Bottom: coherent receiver block diagram.

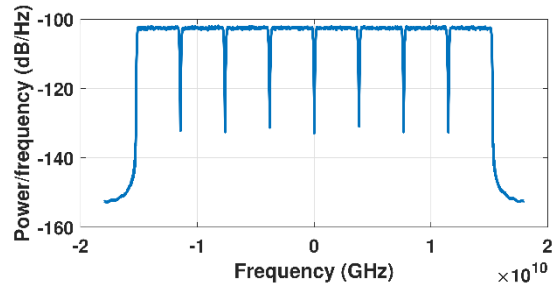


Fig. 2 The spectrum of output signal in a MSC Tx with 32 GHz bandwidth and 250 MHz channel spacing.

## 2- System Model

The diagram of the investigated coherent system is illustrated in the top part of Fig. 1. The optical 32 Gbaud M-QAM signals are generated in electrical domain and then modulated onto an optical carrier at a desired wavelength using an optical modulator Mach-Zehnder modulator (RF/optical converter). Without any loss of generality, calculations are accomplished in baseband. 32-GHz Nyquist-shaped frequency spectrum is divided into  $N_{sc}$  electrical subcarriers for the case of MSC electrical multiplexing. In addition, square-root raised-cosine spectra with  $N_{sc} = 8$  is used as shown in Fig. 2. Independent pseudo-random binary sequences (PRBSs) are used in all MSC channels.

The generated optical signal is fed to the optical channel, consisting of  $N_{span}$  fiber spans with  $L_{span}$  (km) length and each span followed by an erbium-doped fiber amplifier (EDFA), which completely recovers the span loss. On the other hand, EDFA accumulates ASE noise in each span. Therefore, the overall length of the channel is  $L = N_{span}L_{span}$ . Two typical fibers, i.e. non-zero dispersion shifted fiber (NZDSF) and standard single mode fiber (SMF), are used. The fiber parameters (i.e. the

dispersion  $\beta_2$ , the attenuation  $\alpha$ , and the nonlinearity  $\gamma$ ) are reported in Table 1.

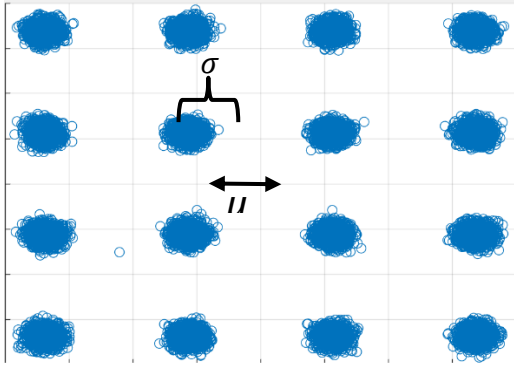


Fig. 3 Typical measured 16-QAM constellation after the dispersion and phase noise compensation in the receiver

The Kerr effect is the origin of nonlinear effects, which are classified as self-channel interference (SPM-like), cross-channel interference (XPM-like) and multi-channel interference (FWM-like). The predominant effect in uncompensated optical systems is FWM or multi-channel interference, which generates new signals through the nonlinear combination of the propagating signals at different frequencies. This nonlinear interference can be modeled as additive noise on the constellation symbols, as shown in Fig. 3 [8].

Table 1: Parameters of simulated systems

Simulated link Parameters	(A)	(B)
Optical fiber	SMF	NZDSF
$\gamma$ (Wkm) <sup>-1</sup>	1.3	2
$\beta_2$ ps <sup>2</sup> /km	-21	-3.38
$\alpha$ dB/km	0.2	0.2288
Signal bandwidth ( $BW$ ) GHz	32	32
Span length ( $L_s$ ) km	100	80
Noise Figure ( $F$ ) dB	5	5
Light frequency ( $\nu$ ) THz	193.1	193.1
PRBS	$2^{18} <$	$2^{18} <$

The ASE noise is the main source of linear noise, which is added by the EDFAs and can be modeled as an additive stationary Gaussian noise with variance [5]:

$$\sigma_{ASE}^2 = N_{span} e^{\alpha L} h \nu F B W \quad (1)$$

where  $F, \nu, h, B W$  are the noise figure of the optical amplifier, the absolute light frequency, the Planck constant, and the reference bandwidth, respectively.

In the bottom part of Fig. 1, a standard coherent receiver is shown, which is used in this paper. The local oscillator (LO) is mixed with the signal in a 90-degree hybrid. In this paper we neglect the effects of LO alignment and linewidth, which is a practical assumption in coherent

system as an advantage of digital signal processing (DSP). Signal components at the output of the two balanced photodetectors are sampled at enough rate for DSP. By using data-aided DSP algorithms linear propagation effects such as CD are completely compensated. Moreover, phase and amplitudes of in-phase and quadrature of received signals are accessible. In dual polarization systems a parallel system is needed at transmitter and receiver, with a different polarization which is completely independent of the other polarization.

### 3- Mathematical Preliminaries

This section presents the principle of signal propagation through the UT optical fiber, together with the relevant basic mathematical equations. Later, the statistical model of the received signal is derived. A new modified signal-to-noise ratio (SNR) is derived based on Johnson  $S_U$  distribution. Then, the deviation of the propagated signal pdf from the Gaussian distribution is measured using the AD and JB Gaussianity tests.

#### 3-1- Gaussianity Tests

For BER evaluation, focusing on the pdf tail is essential and is a better tool for checking pdf. At first glance, the received signal histogram fails accurate Gaussianity tests, particularly when looking at the far tails of the distribution, especially in systems with low BERs. Gaussianity tests are powerful tools for evaluating the extent of deviation of the random sample histogram from Gaussian distribution. The Gaussianity of the symbols pdf is tested by computing the statistics of the JB and AD tests that are described in the following:

AD Test: This test measures the difference between two population sets. The most encouraging point with the AD test is that it focuses upon the difference between the tails of two distributions. If ordered data,  $Y_1, \dots, Y_n$ , come from a distribution with cumulative distribution function  $\Phi$ , the formula for the AD test statistic is,  $A^2 = -n - S$  where [22/]

$$S = \sum_{i=1}^n \frac{2i-1}{n} [\ln(\Phi(Y_i)) + \ln(1 - \Phi(Y_{n+1-i}))] \quad (2)$$

For measuring the distance with Gaussian distribution,  $\Phi(x)$  equals  $1 - Q(x)$

where  $Q(x) = \frac{1}{\sqrt{2\pi}} \int_x^\infty \exp(-\frac{u^2}{2}) du$ .

JB Test: JB test is the second test that is utilized to measure the difference between the histogram of received samples and Gaussianity. Here, the main tools are skewness and kurtosis of the received samples. The test statistic is defined as [23/]:

$$JB = \frac{n}{6} \left( S^2 + \frac{(K - 3)^2}{4} \right), \tag{3}$$

where  $K$  and  $S$  denote kurtosis and skewness of the observed samples, respectively.

It should be mentioned that  $JB$  and  $A^2$  are two metrics and, if the pdf of received samples are Gaussian, the result of both tests will be zero. For non-Gaussian pdf,  $JB$  and  $A^2$  are not zero, and higher values of these metrics mean more distance from Gaussian.

Note that the AD test focuses on the difference between the tails of distributions and the JB test measures Gaussianity using higher order moments.

The system described in Fig. 1 is simulated numerically using the SSFM as a benchmark according to the simulation parameters are reported in Table 1. Linear and nonlinear effects are considered in propagation and then at the receiver linear propagation effects such as CD and constant constellation rotation are compensated. The accuracy of the fit is measured for all symbols of constellation by gathering all symbols to center by subtracting the estimated mean value of each symbols. In each test, the results of real and imaginary parts are summed and plotted for different launch powers.

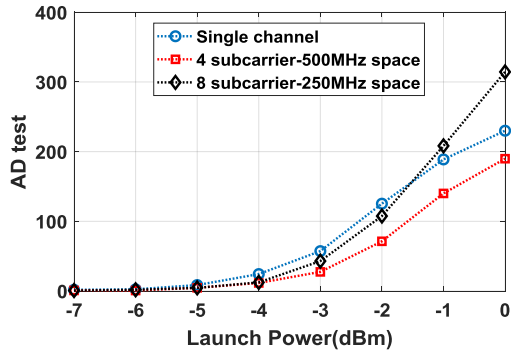


Fig. 4 AD test results for system (B) with  $60 \times 80$  (km) NZDSF link and 4-QAM signals.

The AD and JB tests results are shown in Figs. 4 and 5 for a  $60 \times 80$  (km) NZDSF link (system (B) in Table 1) with 4-QAM signal. Nonlinear threshold is the start point of nonlinear effect where test values diverge from zero (Gaussian pdf). This divergence means that the pdf of received samples changes where nonlinearity begins to affect. The JB and AD test results are again done for system (A) of Table 1 with  $65 \times 100$  (km) SMF link and the results are shown in Figs. 6 and 7. The tails (AD test) and high order statistics (JB test) of the distribution of the received signal are different from Gaussian pdf in nonlinear region and this may significantly affect SER calculations.

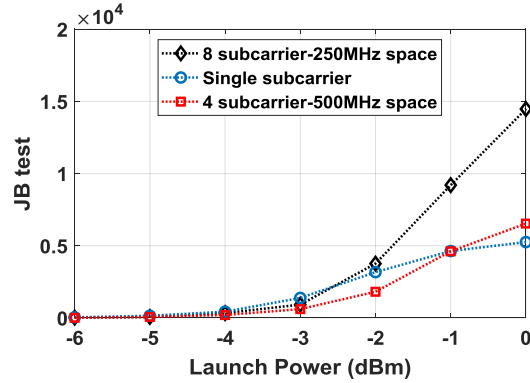


Fig. 5 JB test results for system (B) with  $60 \times 80$  (km) NZDSF link and with 4-QAM signals.

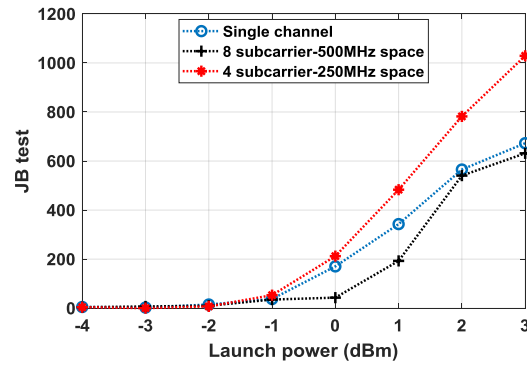


Fig. 6 JB test results for system (A) with  $65 \times 100$  (km) SMF link and with 4-QAM signals.

JB and AD tests are used in the systems with 16-QAM and 64-QAM signals. These two modulations are transmitted over in SMF and NZDSF systems with different span numbers. The results, shown in Figs. 8 and 9, demonstrate that, in a system with NZDSF, received signal distribution deviates from Gaussianity (zero value) at lower powers than SMF, which confirms higher nonlinearity of NZDSF ( $0.002 \text{ (Wkm)}^{-1}$ ) in comparison with SMF ( $0.0013 \text{ (Wkm)}^{-1}$ ). Moreover, over SMF, the results of JB and AD tests show that Gaussianity at the end of span number 8 is more than at span number 6. This can be the effect of high CD in SMF. However, in NZDSF Gaussianity of received signal after 6 spans propagation is more than 8 spans; because nonlinear effect is dominant respect to CD in NZDSF.

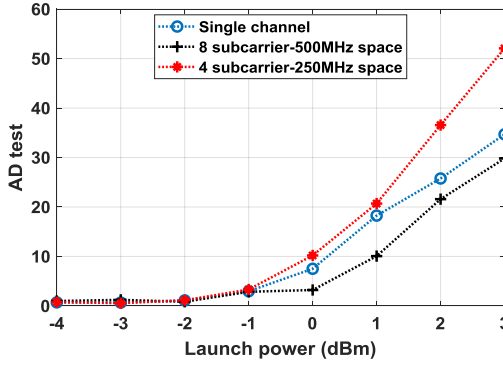


Fig. 7 AD test results for system (A) with  $65 \times 100$  (km) SMF link and with 4-QAM signals.

In the next section, Johnson  $s_U$  distribution is used for SER evaluation, and the obtained results are compared to those achieved using other methods.

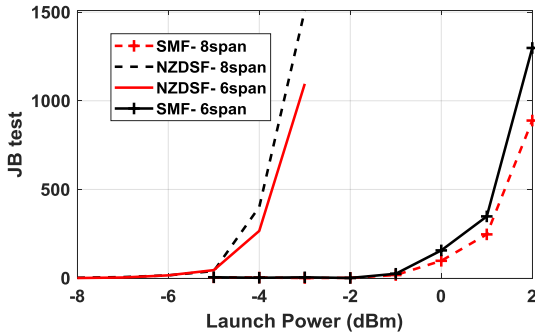


Fig. 8 JB test results for systems (A) and (B) with different span number and dual polarization 16-QAM signals.

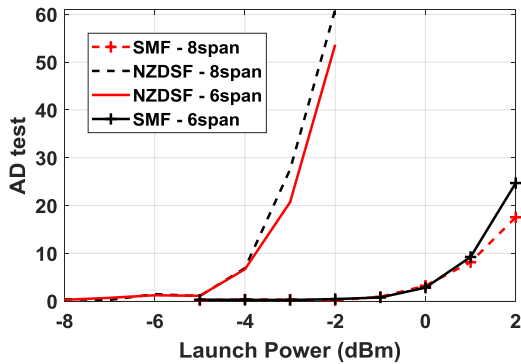


Fig. 9 AD test results for systems (A) and (B) with different span number and dual polarization 16-QAM signals.

### 3-2- New SNR

The BER of any coherent communication system with 4-QAM signals in an AWGN channel is as follows [26/]:

$$BER \approx \frac{1}{2} \operatorname{erfc} \left( \sqrt{\frac{SNR}{2}} \right) \quad (4)$$

and in general for rectangular M-QAM we have

$$SER \approx 2 \left( 1 - \frac{1}{\sqrt{M}} \right) \operatorname{erfc} \left( \sqrt{\frac{SNR}{\frac{2}{3}(M-1)}} \right) \quad (5)$$

It is apparent that using Gray coding:

$$SER = \log_2(M) \times BER \quad (6)$$

SNR in a multi-span optical fiber link has an NLI component which is added to ASE noise and SNR can be written as [24/]:

$$SNR = \frac{P}{\sigma_{ASE}^2 + \sigma_{NLI}^2} \quad (7)$$

where  $P$  is signal power,  $\sigma_{ASE}^2$  and  $\sigma_{NLI}^2$  are ASE noise and nonlinear noise variances, respectively.

Eq. (4) is achieved assuming that the propagated signal in nonlinear optical fiber has a Gaussian pdf. However, it is demonstrated in Figs. 4 - 9 that received signal histogram is not Gaussian after nonlinear threshold and nonlinear region. According to JB test, 3<sup>rd</sup> and 4<sup>th</sup> moments of propagated signal are not zero and we can use them to increase the accuracy of performance estimation, which was proposed also in [25/].

In this way, we proposed in [11] and [16] to use the Johnson  $s_U$  as a four-parameter distribution with two more degrees of freedom with respect to Gaussian pdf for distribution fitting. Johnson  $s_U$  pdf is a transformation of the standard normal pdf [26/] by applying 4<sup>th</sup> and 3<sup>rd</sup> moments of noise statistic. Because of symmetry of FWM effect, 3<sup>rd</sup> moment is set to zero, as mentioned in [11], [16] and we just use the 4<sup>th</sup> moment as an additional degree of freedom to improve the accuracy of system performance prediction. According to Johnson  $s_U$  pdf a close form relationship between BER and SNR can be written as [11]:

$$BER \approx \frac{1}{2} \operatorname{erfc} \left( \delta \sinh^{-1} \left( \frac{\zeta}{\sqrt{2}\lambda} \right) \right) \quad (8)$$

where  $\zeta$ ,  $\lambda$ , and  $\delta$  are parameters of Johnson  $s_U$  distribution that are equal to:

$$\begin{aligned} \zeta &= \hat{\mu}_1 \\ \delta &= \ln(\hat{\omega})^{-\frac{1}{2}} \\ \hat{\lambda} &= \sqrt{\frac{2\hat{\mu}_2}{\hat{\omega}^2 - 1}} \end{aligned} \quad (9)$$

where,

$$\hat{\omega} = \left[ (2\hat{K} - 2)^{\frac{1}{2}} - 1 \right]^{\frac{1}{2}} \quad (10)$$

and

$$\hat{K} = \frac{\hat{\mu}_4}{\hat{\mu}_2^2} \quad (11)$$

$\hat{\mu}_1$ ,  $\hat{\mu}_2$ , and  $\hat{\mu}_4$  are first, second and fourth central moment estimations, respectively [27/]. The hat sign means numerical approximation of parameters. By comparing Eq.(4) and Eq.(6), the following relationships between the SNR and the parameters of the Johnson  $s_U$  distribution are obtained:

$$\sqrt{\frac{SNR}{2}} = \delta \sinh^{-1}\left(\frac{\zeta}{\sqrt{2}\lambda}\right) \quad (12)$$

Therefore,  $SNR/2$  is equivalent to  $h^{-1}\left(\frac{\zeta}{\sqrt{2}\lambda}\right)$ , which can thus be interpreted as a new modified version of SNR. This modified SNR version depends on  $\delta$  as the representative of 4<sup>th</sup> moment in addition to the  $\frac{\zeta}{\lambda}$ , which is the representative of signal and noise powers.

The new SNR can be extended to higher order modulations M-QAM with rectangular constellation like 16-QAM and 64-QAM as follows:

$$\sqrt{\frac{SNR}{\frac{2}{3}(M-1)}} = \delta \sinh^{-1}\left(\frac{\zeta}{\sqrt{\frac{2}{3}(M-1)}\lambda}\right) \quad (13)$$

and the symbol error rate (SER) can be written as:

$$SER \approx 2\left(1 - \frac{1}{\sqrt{M}}\right) \operatorname{erfc}\left(\delta \sinh^{-1}\left(\frac{\zeta}{\sqrt{\frac{2}{3}(M-1)}\lambda}\right)\right) \quad (14)$$

The method of moments is applied to calculate the Johnson  $s_U$  distribution parameters from 2<sup>nd</sup> and 4<sup>th</sup> moments of received signal, numerically.

#### 4- Results and Discussion

Here, three methods are used for estimating the SER as an important parameter of system performance:

- SSFM: as a benchmark to measure the accuracy of the two other methods.

- Gaussian numerical: uses the estimated variance  $\sigma_y^2$ ,  $\sigma_x^2$  and mean  $\mu_y$ ,  $\mu_x$  of the constellation points (see Fig. 3). We assume that in-phase and quadrature parts of received signal are i.i.d [6]. If  $\sigma_y^2$ ,  $\sigma_x^2$  and mean  $\mu_y$ ,  $\mu_x$  belongs to the corners of the constellation for rectangular M-QAM. Based on the Gaussian approximation, Eq. (5) can be used for SER calculation.

- Johnson numerical: pdf parameters  $(\zeta, \lambda, \delta)$  of received sampled signal are needed to calculate SER semi-analytically using the Johnson  $s_U$  distribution. Estimating  $\mu_1$  and  $\mu_2$  is straightforward, similar to the second method, and fourth central moments  $\mu_4$ , is estimated numerically as follows:

$$\hat{\mu}_4 = \frac{1}{N} \sum_{i=1}^N (y_i - \mu_1)^4. \quad (15)$$

where  $y_i$ s are the received samples.

Johnson  $s_U$  distribution parameters can be calculated using Eqs. (9) - (11) according to estimated  $\mu_1$ ,  $\mu_2$ , and  $\mu_4$ . In this method, SER is calculated using Eq. (14) for rectangular distributions.

It should be mentioned that there is an assumption in Eq. (14) and (5) that is the symmetry of distribution which is correct for both Johnson  $s_U$  and Gaussian. Therefore, SER calculation is done just for in-phase or quadrature part.

SER versus launch power estimated using the three methods described above shown in Fig. 10. A 40×80 (km) NZDSF system was simulated, using the parameters reported in Table 1, column (B). According to Fig. 10, in nonlinear region, Johnson  $s_U$  distribution will achieve about 1 dB better power prediction at  $SER = 10^{-3}$  than Gaussian. The simulation of Fig. 10 is repeated for the system (A) with 60×100 (km) SMF spans. This means that there is 60 numbers of 100 km SMF spans. The results shown in Fig. 11 confirm the higher accuracy of proposed method over SMF, as well.

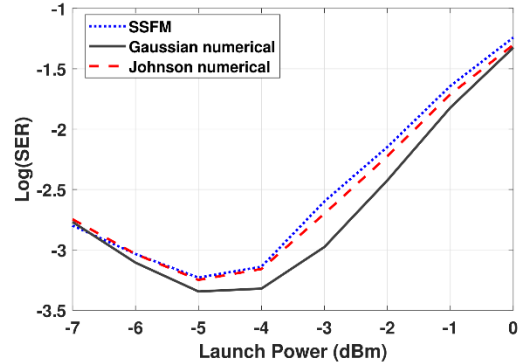


Fig. 10 Performance comparison among three methods in 40×80 (km) NZDSF UT link with parameters of System (B) according to Table 1 and 4-QAM signals.

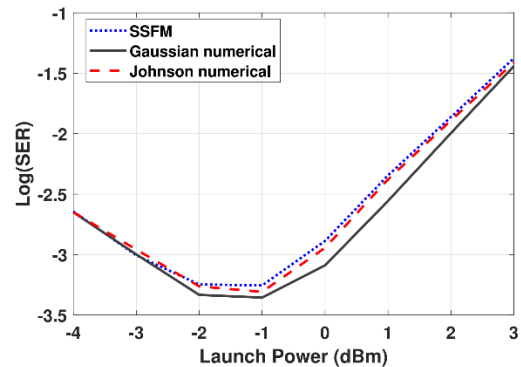


Fig. 11 Performance comparison among three methods in 60×100 (km) SMF UT link with parameters of System (A) according to Table 1 and 4-QAM signals.

SMF has a higher CD and a lower nonlinearity in comparison with NZDSF which results in more Gaussian

received samples and therefore Gaussian based method in Fig. 11 is closer to MC than in Fig. 10.

The accuracy of the proposed method was also assessed in a WDM scenario with 50 GHz spacing. The results over NZDSF (see Table 1, column B) are shown in Fig. 12 where the higher accuracy with respect to the Gaussian based method is confirmed.

In Figs. 13, 14, 15 and 16 Johnson  $s_U$  distribution is used for performance evaluation in MSC systems with different subcarrier number and frequency spacing. The performance improvement is clear in this four figures when the spectrum is divided into 8 and 4 parts with 4 GBaud and 8 GBaud symbol-rate each, respectively. It means that by dividing the spectrum into 4 or 8 parts, nonlinear effects fall down and system can reach more distances with desired performance.

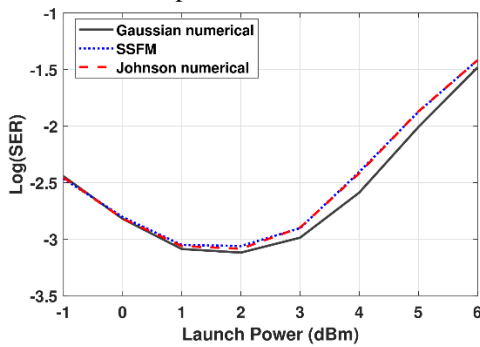


Fig. 12 Performance comparison among three methods in 40x80 (km) NZDSF UT 5-channel WDM link with parameters of System (B) according to Table 1 for each channel and 4-QAM signals.

By comparing Figs.13 and 14, it can be concluded that 8-subcarrier spectrum have more robustness than 4-subcarrier spectrum against nonlinearity. It is also apparent that the proposed Johnson  $s_U$  based method is more accurate than the Gaussian method in all analyzed configurations and SER prediction error is reduced to less than 0.1 order of magnitude in SMF links. According to Figs. 13-16, system performance can improve of about one and more than one order of magnitude in SMF and NZDSF links, respectively.

The performance evaluation of MSC is again done for system (B) scenario, as is shown in Figs. 15 and 16. In MSC system with 8 subcarriers and 500 MHz spacing of Figs. 15 and 16, there is more than 0.5 order of magnitude SER deviation at -2 dBm launch power and more than 1.5 dB power prediction error using Gaussian based method at  $SER = 10^{-3.5}$ . The frequency spacing in Fig.16 decreased to 250 MHz, which can increase nonlinear effect. It is also shown that the proposed Johnson  $s_U$  based method is more accurate than the Gaussian methods in NZDSF based links.

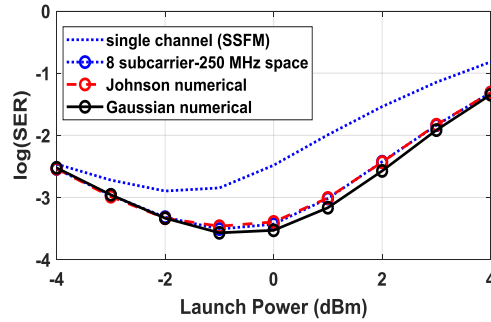


Fig. 13 Performance comparison among three methods in 65x100 (km) SMF UT link with parameters of System (A) according to Table1 and 4-QAM signals. Blue dotted curves belong to numerical SSFM.

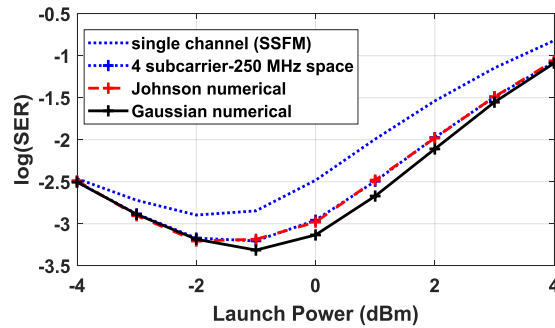


Fig. 14 Performance comparison among three methods in 65x100 (km) SMF UT link with parameters of System (A) according to Table1 and 4-QAM signals. Blue dotted curves belong to numerical SSFM.

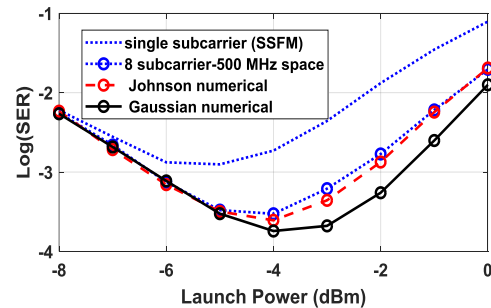


Fig. 15 Performance comparison among three methods in 45x80 (km) NZDSF UT link with parameters of System (B) according to Table1 and 4-QAM signals. Blue dotted curves belong to numerical SSFM.

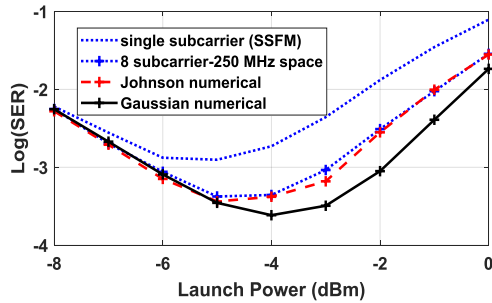


Fig. 16 Performance comparison among three methods in 45×80 (km) NZDSF UT link with parameters of System (B) according to Table1 and 4-QAM signals. Blue dotted curves belong to numerical SSFM.

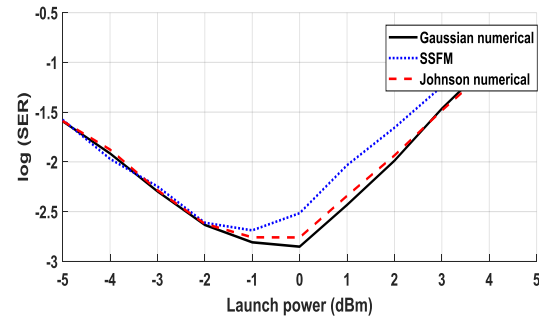


Fig. 18 Performance comparison among three methods in 3×100 (km) SMF UT link with parameters of System (A) according to Table1 with dual polarization 64-QAM signals.

SER versus launch power estimated using the three methods, described above, is shown in Figs. 17 and 18. A 10×100 (km) and a 3×100 SMF based link is simulated, using the parameters reported in Table 1, column (A). It can be seen from Fig. 17 and 18 that, in nonlinear region, Johnson  $s_{\mathcal{U}}$  distribution works better than Gaussian, and the performance fits to the SSFM results more accurately. The nonlinear effects of high order modulation cause an equalization error that corrupts the moment estimation and that causes a gap between SSFM and two other methods. For tackling with this problem, analytical methods can help, which will be done in future works.

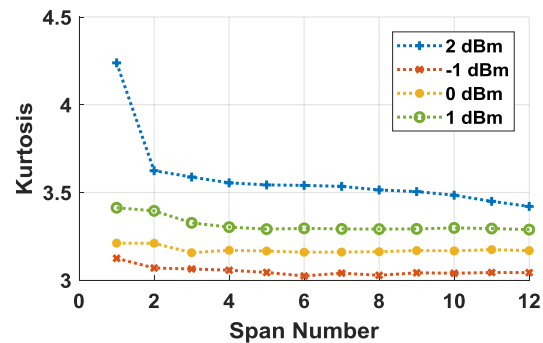


Fig. 19 Kurtosis comparison in 10×100 (km) SMF UT link with parameters of System (A) according to Table1 with dual polarization 16-QAM signals. Kurtosis for a Gaussian data set is 3.

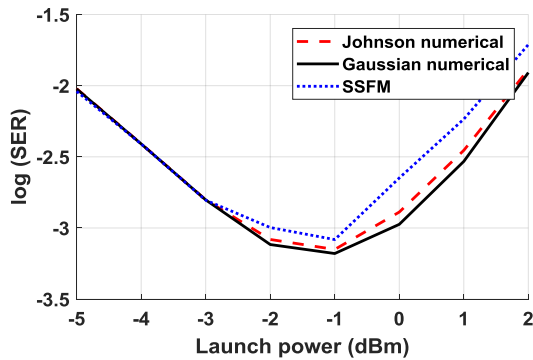


Fig. 17 Performance comparison among three methods in 10×100 (km) SMF UT link with parameters of System (A) according to Table1 with dual polarization 16-QAM signals.

In addition, CD is another parameter that affects Gaussianity of signal i.e. the signal is dispersed by increasing the span number. By increasing the span number, received signal kurtosis starts to converge to 3 (kurtosis of a Gaussian data set), which is shown in Fig.19 for 4 different powers. At high powers, kurtosis value is higher due to nonlinear effect.

### 5- Conclusion

The statistics of the propagated signal in optical fiber transmission system can be affected by nonlinear effects which have a critical role in system performance calculation. Nonlinear effects deviate propagated signal probability distribution from the Gaussian distribution (which is a typical assumption in modeling of optical systems) when the launch power increases. In this paper, two JB and AD tests have been used to measure the deviation of propagated signal at different powers, modulations, and span numbers. As a result of the mentioned tests, propagated signal distribution starts to deviate from Gaussian after the nonlinear threshold. Therefore, the performance prediction methods based on the Gaussian assumption are not accurate in the nonlinear region. This paper extended the use of the Johnson  $s_{\mathcal{U}}$  distribution for performance evaluation of coherent optical systems with different kinds of signals; single carrier M-QAM signals, multi-subcarrier QPSK transmission systems are considered because of their higher nonlinear robustness in comparison with single-carrier systems. We also analyzed the performance of proposed method in dual

polarization systems. Monte-Carlo simulation results were used for verification of the proposed semi-analytical approach, which is more accurate in different scenarios in

### Acknowledgments

We would like to thank Prof. Gabriella Bosco from Technical University of Turin for her time, technical supports and valuable comments.

### References

- [1] P. Poggiolini and Y. Jiang, "Recent advances in the modeling of the impact of nonlinear fiber propagation effects on uncompensated coherent transmission systems," *Journal of Lightwave Technology*, Vol. 35, No 3, 2017, pp. 458-480.
- [2] P. Poggiolini, G. Bosco, A. Carena, V. Curri, Y. Jiang, F. Forghieri, "The GN model of fiber non-linear propagation and its applications," *Journal of Lightwave Technology*, Vol. 32, No. 4, 2014, pp. 694-721.
- [3] P. Poggiolini, Y. Jiang, A. Carena, F. Forghieri, Analytical Modeling of the Impact of fiber Non-Linear Propagation on Coherent Systems and Networks, in *Enabling Technologies for High Spectral-efficiency Coherent Optical Communication Networks*, Xiang Zhou, Chongjin Xie editors, chapter 7, pp. 247-310, ISBN: 978-1-118-71476-8, Wiley, Hoboken (NewJersey), 2016.
- [4] R.-J. Essiambre, G. Kramer, P. J. Winzer, G. J. Foschini, and B. Goebel, "Capacity limits of optical fiber networks," *Journal of Lightwave Technology*, Vol. 28, No 4, 2010, pp. 662–701.
- [5] G. P. Agrawal, *Nonlinear fiber optics*, Academic Press, 2007.
- [6] L. Beygi, E. Agrell, P. Johannisson, M. Karlsson, and H. Wymeersch, "A discrete-time model for uncompensated single-channel fiber-optical links," *IEEE Transaction on Communication*, Vol. 60, No 11, 2012, pp. 3440-3450.
- [7] R. Dar, M. Feder, A. Mecozzi, and M. Shtaif, "Properties of nonlinear noise in long, dispersion-uncompensated fiber links," *Optics Express*, Vol. 21, No 22, 2013, pp. 25685-25699.
- [8] A. Carena, V. Curri, G. Bosco, P. Poggiolini, and F. Forghieri, "Modeling of the impact of nonlinear propagation effects in uncompensated optical coherent transmission links," *Journal of Lightwave Technology*, Vol. 30, No 10, 2012, pp.1524-1539.
- [9] P. Serena, A. Bononi, and N. Rossi, "The impact of the modulation dependent nonlinear interference missed by the gaussian noise model," *ECOC 2014*.
- [10] S. T. Le, K. J. Blow, V. K. Mezentsev, and S. K. Turitsyn, "Bit error rate estimation methods for QPSK CO-OFDM transmission," *Journal of Lightwave Technology*, Vol. 32, No 17, 2014, pp. 2951-2959.
- [11] S. S. Kashef, P. Azmi, G. Bosco, M.D. Matinfar, and D. Piloni, "NonGaussian Statistics of CO-OFDM Signals after Non-Linear Optical Fiber Transmission," *IET optoelectronics*, Vol. 12, No 3, 2017, pp. 150 – 155.
- [12] A. Carena, G. Bosco, V. Curri, Y. Jiang, P. Poggiolini, and F. Forghieri, "On the accuracy of the GN-model and on analytical correction terms to improve it," *arXiv preprint arXiv:1401.6946*, 2014.
- [13] G. Gao, X. Chen, and W. Shieh, "Analytical expressions for nonlinear transmission performance of coherent optical OFDM systems with frequency guard band," *IEEE Photonics Technology Letters*, Vol. 30, No 15, 2012, pp. 2447-2454.
- [14] D. Uzunidis, C. Matrakidis, and A. Stavdas, "An improved model for estimating the impact of FWM in coherent optical systems," *Optics Communications*, Vol. 378, 2016, pp. 22-27.
- [15] A. Carena, G. Bosco, V. Curri, Y. Jiang, P. Poggiolini, and F. Forghieri, "EGN model of non-linear fiber propagation," *Optics Express*, Vol. 22, No 13, 2014, pp. 16335-16362.
- [16] S. S. Kashef and P. Azmi, "Performance Analysis of Nonlinear Fiber Optic in CO-OFDM Systems with High Order Modulations," *IEEE Photonics Technology Letters*, Vol. 30, No 8, 2018, pp. 696-699.
- [17] S. S. Kashef, G. Bosco, and P. Azmi, "Johnson S U Distribution in Uncompensated QPSK Coherent Optical Transmission Systems." *ICEE*, 2019, pp. 1284-1288.
- [18] D. Uzunidis, C. Matrakidis, and A. Stavdas, "Analytical FWM expressions for coherent optical transmission systems," *Journal of Lightwave Technology*, Vol. 35, No13, 2017, pp. 2734-2740.
- [19] D. Uzunidis, C. Matrakidis, and A. Stavdas, "Closed-form FWM expressions accounting for the impact of modulation format," *Optics Communications*, Vol. 440, 2019, pp.132-138.
- [20] F. P. Guiomar, A. Carena, G. Bosco, L. Bertignono, A. Nespola, and P. Poggiolini, "Nonlinear mitigation on subcarrier-multiplexed PM-16QAM optical systems," *Optics Express*, Vol. 25, No 4, 2017, pp. 4298-4311.
- [21] F. Buchali, W. Idler, K. Schuh, L. Schmalen, T. Eriksson, G. Bcherer, P. Schulte, and F. Steiner, "Study of electrical subband multiplexing at 54 GHz modulation bandwidth for 16QAM and probabilistically shaped 64QAM," *ECOC*, 2016, pp. 4951.
- [22] R. D'Agostino, *Goodness-of-fit-techniques*, Routledge, 2017.

- [23] C.M. Jarque, and A. K. Bera, "A test for normality of observations and regression residuals," *International Statistical Review/Revue Internationale de Statistique*, 1987, pp. 163-172.
- [24] A. Carena, V. Curri, G. Bosco, P. Poggiolini, F. Forghieri, "Modeling of the Impact of Non-Linear Propagation Effects in Uncompensated Optical Coherent Transmission Links," *Journal of Lightwave Technology*, Vol. 30, No 10, 2012, pp. 1524-1539.
- [25] P. Jenneve, P. Ramantanis, J.C. Antona, G. de Valicourt, M. Mestre, H. Mardoyan, and S. Bigo, "Pitfalls of error estimation from measured nongaussian nonlinear noise statistics over dispersion-unmanaged systems," *ECOC 2014*.
- [26] W. P. Elderton and N. L. Johnson, *Systems of frequency curves*, Cambridge University Press London, 1969.
- [27] I. D. Hill, R. Hill, R. L. Holder, "Algorithm AS 99: Fitting Johnson curves by moments," *J. the royal statistical society. Series C (Applied statistics)*, vol. 25, no. 2, 1976, pp 180-189.

**Seyed Sadra Kashef** received the B.S. degree in Telecommunication Engineering from Tabriz University, Tabriz, Iran in 2012, M.S. degree Ph.D. in Telecommunication Engineering from Tarbiat Modares University, Tehran, Iran, in 2014 and 2018, respectively. Currently he is assistant professor in Urmia University, Iran. Her research interests include Optical communications, machine learning, communication theory, estimation theory.

**Paeiz Azmi** was born in Tehran, Iran, in April 1974. He received the B.Sc., M.Sc., and Ph.D. degrees in electrical engineering from the Sharif University of Technology (SUT), Tehran, in 1996, 1998, and 2002, respectively. From 1999 to 2001, he was with the Advanced Communication Science Research Laboratory, Iran Telecommunication Research Center (ITRC), Tehran, where he was with the Signal Processing Research Group, from 2002 to 2005. Since September 2002, he has been with the Electrical and Computer Engineering Department, Tarbiat Modares University, Tehran, where he became an Associate Professor, in January 2006, and is currently a Full Professor. His current research interests include modulation and coding techniques, digital signal processing, wireless communications, radio resource allocation, molecular communications, and estimation and detection theories.